UDK 669.018:621.793.7:669.14.018.8:544.3.032
Original scientific article/Izvirni znanstveni članek

ISSN 1580-2949
MTAEC9, 52(5)653(2018)

INFLUENCE OF THE PROCESS PARAMETERS ON HIGH-VELOCITY OXYGEN-FUEL-SPRAYED 75Cr_3C_2-25NiCr COATINGS

VPLIV PROCESNIH PARAMETROV NA IZDELAVO 75Cr_3C_2-25NiCr PREVLEK S POSTOPKOM NAPRŠEVANJA PRI VISOKIH HITROSTIH

BalaGanesh Nagulan, SenthilKumar Thamilkolundu, Chandrasekar Murugesan

Anna University, University College of Engineering, Department of Mechanical Engineering, Bit-Campus, Tiruchirappalli 620024, Tamil Nadu, India
balaganeshnagulan@gmail.com

Prejem rokopisa – received: 2017-12-28; sprejem za objavo – accepted for publication: 2018-05-25

doi:10.17222/mit.2017.224

In this work 75Cr_3C_2-25NiCr powder was sprayed on stainless steel with various pressures and powder-feed rates utilizing the HVOF method. The microstructure of the coating and the micro-hardness and porosity, micro-hardness, indentation fracture toughness, adhesion strength and wear resistance at 490 °C of the surface coatings were examined. The outcomes demonstrated that HVOF sprayed 75Cr_3C_2-25NiCr coatings had low porosity, high micro-hardness and enough adhesion strength. The powder feed rate had an evident impact on the porosity, micro-hardness and indention fracture toughness of the coatings, and the coating sprayed under the powder feed rate of 35 g/min had the ideal execution. The wear-resistance test showed that the HVOF indicated that the 75Cr_3C_2-25NiCr surface coatings had great influence on the wear resistance at 490 °C, in which the coating sprayed at the powder flow rate of 35 gram/min had the best wear resistance because of its thick and dense structure and having enough fracture toughness.

Keywords: 75Cr_3C_2-25NiCr, coating, adhesion strength, powder feed rate, wear resistance

Avtorji v članku opisujejo, kako so prah zlitine 75Cr_3C_2-25NiCr naprševali na nerjavno jeklo s postopkom plamenskega naprševanja pri visokih hitrostih (HVOF; angl.: High-Velocity Oxy-Fuel Method). Pri tem so uporabili različne tlake oz. hitrosti nanašanja kovinskega prahu. Nato so preučevali mikrostrukture nastalih prevlek, njihovo mikrotrdoto in poroznost, lomno žilavost, določeno z metodo vtiskovanja indenterja (piramide), adhezijsko trdnost ter odpornost proti obrabi pri 490 °C. Rezultati so pokazali, da imajo s HVOF postopkom izdelane 75Cr_3C_2-25NiCr prevleke majhno poroznost, visoko mikrotrdoto in zadovoljivo adhezijsko trdnost. Hitrost nanašanja (naprševanja) kovinskega prahu je imela opazen vpliv na poroznost, mikrotrdoto in lomno žilavost prevlek. Idealna hitrost naprševanja je bila 35 g/min. Pri teh pogojih je imela 75Cr3C2-25NiCr prevleka tudi največjo odpornost proti obrabi pri 490 °C, ker je bila tako izdelana prevleka primerno debela, z ustrezno gosto strukturo in zadovoljivo lomno žilavostjo.

Ključne besede: 75Cr_3C_2-25NiCr, prevleka, adhezijska trdnost, hitrost naprševanja, odpornost proti obrabi.

1 INTRODUCTION

Cermet coatings are generally utilized as a part of modern applications against tribological degradation, even in the eroding condition, because of their high hardness and the great resistance of the utilized metal matrix. Chromium-carbide-based materials are, by and large, utilized to create hard coatings for high-temperature wear applications, including sliding, fusing, scraped spot, and disintegration in the powder generation industry, avionic business, oil refining industry, heat-treatment rolls, and coal-consuming heater tubes.[1,2] The chromium-carbide nickel chromium (75Cr_3C_2-25NiCr) cermet coatings have been broadly practiced in industry, due to the profitablemix of the 75Cr_3C_2 phase of ceramic with great wear resistance and the 75NiCr metal stage, which gives high oxidation resistance at high temperature.[3,4] The procedure of high-speed oxygen fuel (HVOF) splash ends up being the most encouraging procedure, which implies it is desirable over store cermet coatings, for example, Cr_3C_2-NiCr and WC–Co. This method joins high-speed powder particles with low temperature to develop a thick and firmly adhesive coating with residual stress and low oxidation.[5] Coatings kept by the HVOF procedure show high density, low porosity, and brilliant adhesion strength, with substantially more carbide particles held in the matrix in contrast to those saved by the plasma splashing process. It has been accounted for that HVOF-sprayed Cr_3C_2-NiCr coatings display great wear resistance and erosion resistance in different high-temperature conditions.[6–9] Numerous specialists revealed that the execution and microstructure of cermet coatings was overwhelmingly impacted by the spray conditions.[10] The research of Qun Wang et al.[11] outlined that a difference in the spraying parameters demonstrated little impact on the phase structure of the WC–12Co coatings, however, it affected different performances, for example, hardness, porosity, fracture toughness, and the per-pass thickness of the coatings. It

additionally reasoned that the arrangements of significance of coating parameters on the performances of coatings are as per the following: fuel flux > spray distance > feed rate > oxygen flow for hardness; spray distance > fuel flow > feed rate > oxygen flow for porosity; oxygen flux > kerosene flux > feed rate > spray distance for fracture toughness; and feed rate > spray distance > oxygen flow > kerosene flow for per-pass thickness. H. Fukutome et el.[12] examined the impact of a low proportion of oxygen to propene on the phase and abrasive wear of a HVOF Cr_3C_2-20%NiCr coating and presumed that the best wear performance could be acquired when the flow proportion moved towards the chemical ratio, above which the Cr_2O_3 would exist. It has been accounted for that the hardness, fracture toughness of the matrix, fortifications, and the interfacial strength of the support/matrix are the most vital mechanical variables that decide the wear resistance and the disappointing properties of cermet-based coatings.[13,14] The impact of fracture toughness on coating wear performance was explored generally. High fracture toughness was useful for the wear resistance of the coatings.[14] Gang Chang Ji announced the evacuation of carbide particles in the coating was chiefly responsible for the abrasive wear of the coating. The substance and molecule size of the Cr_3C_2 carbides were the two key variables controlling the abrasive wear of the HVOF-coated Cr_3C_2-NiCr coatings.[15,16] In the present work, three levels of 75Cr_3C_2-25NiCr coatings produced by HVOF were coated under various powder feed rates utilizing Hipojet 2700 system, Jodhpur, India, Aum Surface Technologies, Bangalore. All the coatings were analysed by X-ray diffraction (XRD), optical microscope, image analyser, scanning electron microscope (SEM) including energy-dispersive spectroscopy (EDS), micro-hardness analyser, and nano-indenter. The wear resistance and wear mechanisms of the 75Cr_3C_2-25NiCr coatings at 490 °C were researched and investigated.

2 EXPERIMENTAL PART

The 75Cr_3C_2-25NiCr feedstock powders of circular shape and a grain size of approx. 45 μm to 10 μm were coated on SS304 stainless-steel substrates. Three sorts of coatings were acquired by HVOF and the spraying parameters were recorded as **Table 1**. The Hipojet 2700 was utilized to obtain the coating. The powder was axially fed via the air. Prior to spraying, the stainless-steel plates of 10 mm × 10 mm × 5 mm were grit-blasted with alumina to accomplish a surface roughness (R_a) of around 7 μm to 8 μm and after that cleaned in a ultrasonic bath of acetone in order to improve the adhesion strength between the coatings and substrate. The substrates are shown in **Figure 7**. The thickness of the as-sprayed coatings was around 200 μm.

Table 1: Spray parameters of the three coatings.

Coating	Powder Feed Rate (g/min)	Fuel (LPM)	Oxygen (LPM)	Spray Distance (mm)
A	30	30	150	200
B	35	33	160	225
C	40	36	170	250

The wear performance of the coated specimens measurements, i.e., 10 mm × 10 mm × 5 mm, was tested using a ball-on-disk (BOD) high-temperature wear analyser. Before the test, the coated examples were cleaned and afterward cleaned ultrasonically with acetone and alcohol. The coated specimens were mounted immovably in the example holder and were permitted to be pressed against the rim of the rubber wheel with a normal pressure by applying a known dead weight (21 N). The test was performed at 490 °C for 3550 s to acquire the friction coefficient of the coatings. The wear counterpart was the WC ball, whose width was 6 mm. The wear rate of the coatings was measured by volume wear loss. After the HVOP spraying, the examples were cut into pieces of 10 mm × 10 mm × 5 mm and again cleaned ultrasonically with acetone and alcohol. The cross-sectional micrograph of the coatings was obtained by optical microscopy. The well-worn surface of the coatings was likewise analysed by SEM/EDS and a surface profiler. The porosity was measured with an imaging apparatus. For each specimen, the mean estimation of the eight readings was ascertained for measuring the porosity. The X-ray diffraction (XRD) investigation of the coating was made at first glance with a Vega3 Tescan, Czech Republic. It is operated at 40 kV and 40 mA, utilizing Cu-K_α as radiation. The composition of the coating powder were examined utilizing Energy-Dispersive X-beam Spectroscopy (EDS) and an Oxford Instruments framework, crest potentially excluded 3.698 KeV, handling alternative: all components broke down, number of cycle = 3 The bond strength of the coatings was tested with the ASTM adhesion test standard.[17] The microhardness of the as-sprayed coatings was measured by a Wilson-402 MVD microhardness tester at 1 kg and for a stacking span of 15 s. The normal estimation of the five readings for every example was figured. The indentation fracture of the coating toughness was tried by indentation mechanical assembly of Vickers indenter Model: VH 1150, Wilson. The indentation was made on the cross-segment of the coatings in the mid-plane locale to limit the edge and interface impact. The indenter was stacked so one of the even diagonals was parallel to the interface of the coating and substrates. A weight of 2 kg was connected for a dwell time of 20 s at the settled rate. A nano-indention test was used on the surface of coating with a G200 Nano-indenter For each example, 15 readings were obtained on the cleaned surface using a similar parameter, and the indention was acquired by a microscope. Meanwhile, the empty to stack curve was acquired.

3 RESULTS

The XRD examples of the 75Cr_3C_2-25NiCr powder and three coatings are shown in **Figure 1**. Peaks of carbides (Cr_3C_2) and binder phase (NiCr) were observed in both the powder and coatings. The carbides phase of Cr_7C_3 was found in the coating, which was framed by the decarburization of Cr_3C_2. In the examination of the powder and coatings, there was an exceptionally wide peak focused cycle 43° in the example of the coatings. All the peaks of nickel had a strong arrangement and the Cr_3C_2 was noticeably expansive, and an extremely wide peak revolved at around 43° showed up in the as-sprayed state of three coatings. The extremely wide peak demonstrated the arrangement of an undefined phase because of the high cooling rate of HVOF process. In this way, it was demonstrated that the nickel–chromium alloy and some Cr_3C_2 carbide were dissolve and some amorphous phase framed. The comparable outcomes were likewise detailed in those past investigations observed the change of the Cr_3C_2 phase to the $Cr_{23}C_6$ phase while spraying 75Cr_3C_2-25NiCr powder by the jet procedure. Nonetheless, this change was not found in this examination. One conceivable reason was that the living arrangement time of the particles in the flame was significantly less for the spraying system with fluid fuel.[18,19,20] Three XRD examples of coatings were about the same and demonstrated little decarburization of the Cr_3C_2, which showed little impact of spraying parameters on the coating phase structure. It outlined the coating-B had more Cr_3C_2 stage, which implied moderately little decarburization of the Cr_3C_2 into Cr_7C_3 of the coating B. It has been accounted for that Cr_3C_2 and binder NiCr were the real phases of HVOF sprayed chromium carbide-based coating, and the decarburization of Cr_3C_2 into Cr_7C_3 or $Cr_{23}C_6$ did not have an inconvenient impact on the wear resistance of the coatings.[21]

The cross-sectional micrographs of three coatings are shown in **Figure 2**. The micrographs demonstrated that the three coatings had comparative permeable microstructures and the chromium carbide particles were encompassed by the matrix phase in the coatings. The thickness of the coatings is around 200 μm. No splits can be seen on the cross-sections of the coatings. It is accounted for that there are two sorts of pore in the HVOF sprayed coating. One is striated and the other is dispersed consistently all through the covering.[22] Comparable pores could likewise be found in the present research. The coatings had a thick structure and the carbides conveyed consistently in the coating. It could be seen that the covering B was more dense and uniform than others, which was the least permeable of the three coatings.

The coating porosity is an essential issue in the thermal spraying strategy as it identifies with various coating mechanical properties.[23] The metallographic examination of the coatings demonstrates a low porosity. As shown in **Table 2**, HVOF-sprayed 75Cr_3C_2-25NiCr coatings have

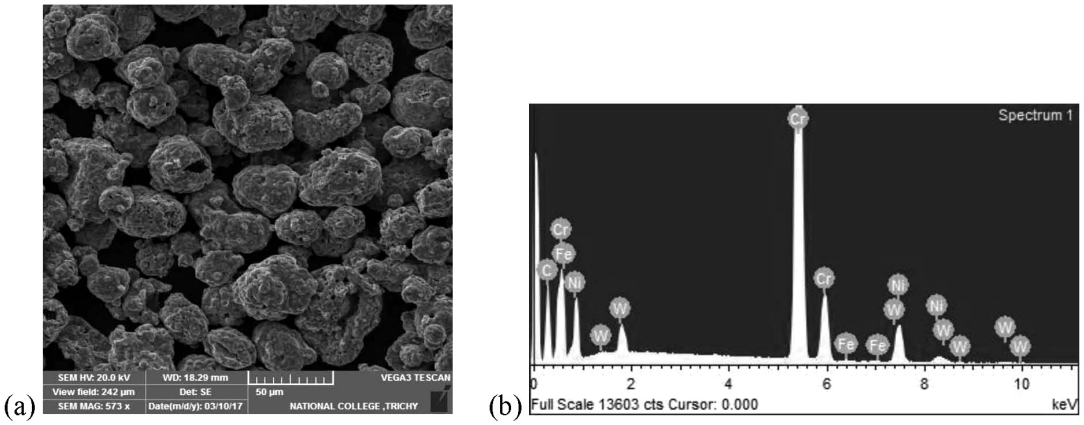

Figure 1: a) SEM Image of Cr_3C_2-NiCr powder, b) XRD pattern of powder

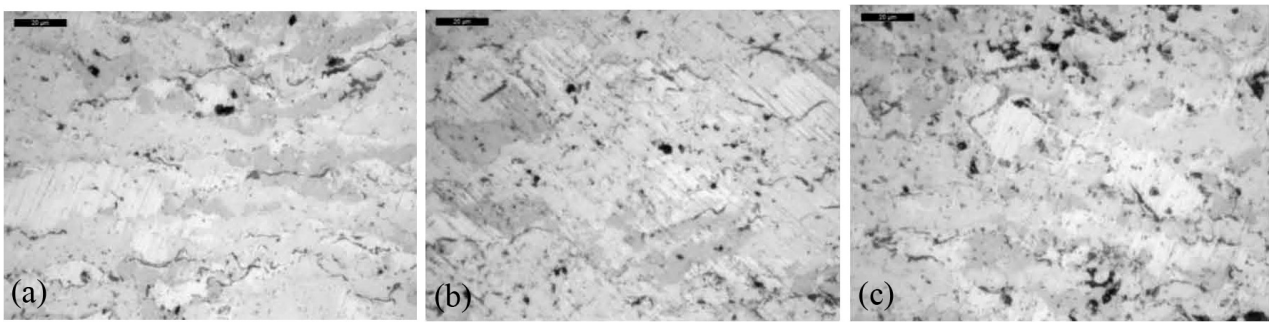

Figure 2: Micrographs of the coatings: a) coating A, b) coating B, c) coating C

low porosity. It reflects that coating B has the least porosity among the three coatings. It is accounted for that the HVOF procedure shows the most reduced porosity caused by its high impact velocity, contrasting with the other spraying systems, for example, electric arc, flame, plasma spraying, and detonation gun.

Table 2: Characteristics of the three coatings.

Coating	Porosity (%)	Adhesion strength (mpa)	Indention fracture toughness (mPa $m^{1/2}$)	Hardness (hv)
A	0.9	62	4.14	875.4
B	0.60	73.7	5.59	884.2
C	1.14	62.2	4.89	862.3

The microhardness estimations of the coatings are given in **Table 2**. The outcomes demonstrate that the HVOF sprayed 75Cr_3C_2-25NiCr coating displays a high microhardness (around 800 HV). In like manner, high hardness is of advantage to wear protection in light of the fact that the hard carbide could balance the external stress successfully. The adhesive strength is a standout amongst the most vital factors in thermal spray coating since it directly identifies with the coating.[24] The adhesion of coating to the substrate was explored by the tensile test. As **Table 2** appears, the adhesion strength of HVOF sprayed Cr3C2-25NiCr coating could accomplish more than 60 MPa. The coatings indicate better adhesive performance, perhaps in light of the fact that the particle was immovably inserted into the substrate at high speed by utilizing HVOF spraying and the residual compression could likewise be a reason. It has been accounted for that the higher adhesion strength (>80 MPa) of coatings could be achieved in both the HVOF and the HVAF frameworks.[25] As **Table 1** appears, the fuel flow and powder feed are close and the spraying parameters of the three coatings are for the most part extraordinary in the powder feed rate. The proportion of the combustion weight to the stream of fuel is 0.417 for every one of the coatings. Along these lines, it is important to examine the impact of the powder feed rate on the coating's properties. **Figure 3** demonstrates the impact of powder feed rate on the coating's properties. As **Figure 3** shows, it could be reasoned that the powder feed rate greatly affects the porosity, adhesion strength, and fracture toughness of the coating. With the feed rate diminishing, the molten level of the spray particles expanded, which brought about the expansion of the hardness and the abatement of the porosity. In the interim, the aggregate particles kept on the substrate diminished and it brought about a reduction of the per-pass thickness.[11] In this way, in the present examination, the coating kept at a powder feed rate of 35 g/min had the optimal basic properties.

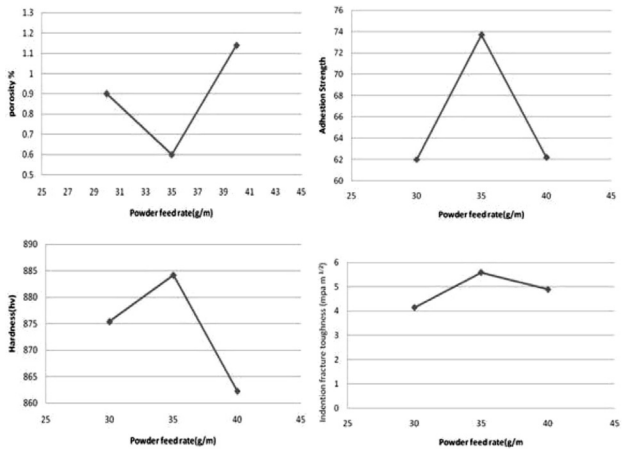

Figure 3: Effect of powder feed rate on: a) porosity, b) microhardness, c) adhesion strength and d) indention fracture toughness of 75Cr_3C_2-25NiCr coating

Figure 4 demonstrates the regular indentations on the transverse area with in-plane cracks for the three coatings, separately. Because of the qualities of thermally sprayed coatings, the cracks parallel to the coating substrate interface are less likely to be formed in comparison with those in the perpendicular direction.[26] It comes from the elongated nature of the splats and the residual stress fields introduced.[20] The length of crack c, from the middle to the indent, was utilized for deciding the fracture toughness of the coatings. The fracture toughness, KIC, was computed through the accompanying conditions.[13]

$$kc = 0.193\ (HVd)(E/HV)2/5(a) - 1/2,\ c/d \leq 2.5 \quad (1)$$

$$kc = 0.711\ (HVd1/2)(E/HV)\ (a) - 3/2,\ c/d \geq 2.5 \quad (2)$$

where E is the Young's modulus and HV is the Vickers hardness, d is the half diagonal of the Vickers indentation. The radial crack length c, is equal to a, the

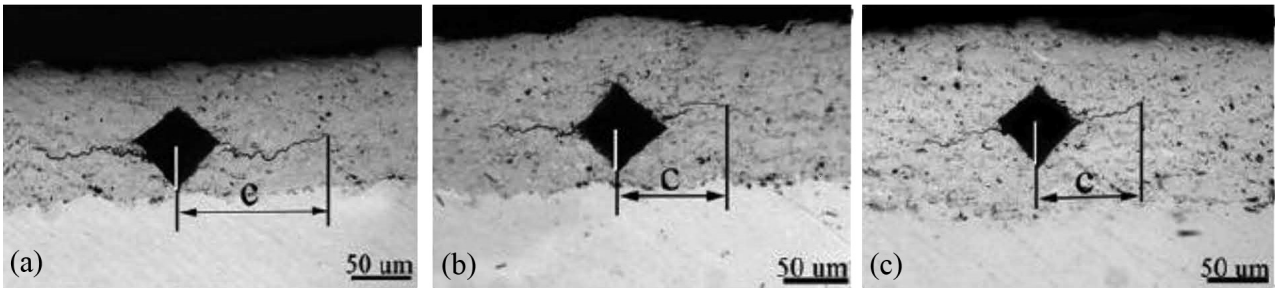

Figure 4: Micrographs of Vickers indentations of coatings A, B, C

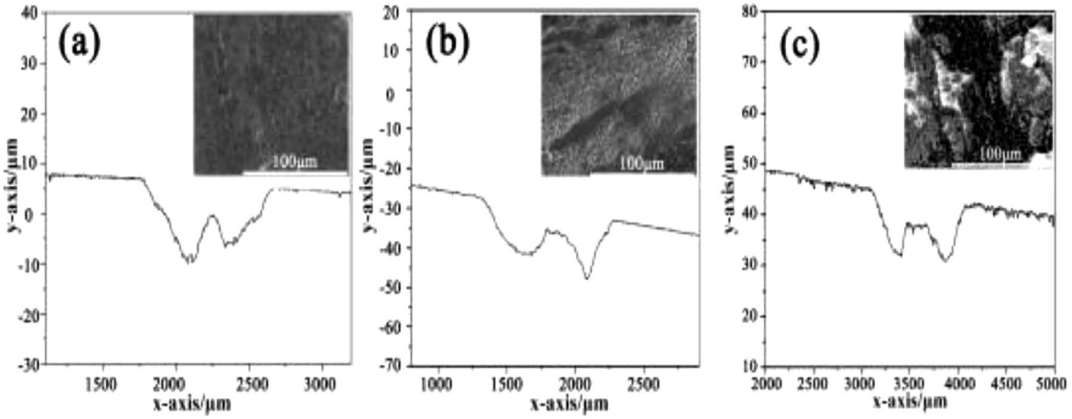

Figure 5: Micrographs of the worn surfaces of coatings A, B, C

indentation crack length *d*, the half diagonal of the Vickers indentation. Both the Vickers diagonal and crack length are analysed and measured from an optical image. The Young's modulus of the coating was calculated by a nano-indenter. Five readings were tested for each sample and the typical fracture toughness values of the coatings are shown in **Table 3**. The fracture toughness is of the three $75Cr_3C_2$-25NiCr coatings. It has been indicated that the scatter of fracture toughness was also observed in the HVOF thermal sprayed coatings, which indicated the microstructural properties of non homogeneous coatings.[26] The scatter was also brought into being in this work and the result indicates, compared with the other coatings, that coating B had superior fracture toughness, which may be endorsed by its lowest porosity.

Table 3: The wear rates of the coatings.

Coating type	Friction coefficient	Wear rate (10–15 m^3/N m)
A	0.34	7.06
B	0.31	6.48
C	0.37	7.32

There are three possibilities of the nano-indenter pressed into the surface, namely, hard phase, middle zone between hard phase and binder phase, binder phase or defect. The micrographs of the nano-indentation showed these three possibilities, which showed a larger indentation successively. There are hard phase of higher hardness and smaller indentation on the binder phase and fewer defects in coating B. As **Figure 5** shows, there are hard phases of higher hardness and smaller indentation on binder phase and fewer defects in coating B. which demonstrates a dense structure with few defects and more hard carbide content.

In addition, special interest is given to the unload-to-load-ratio of the nano-indentation, which represents the ratio between the total work (Wt) done and the recovered (elastic) work during indentation.[27] It can separate the indentation work into elastic (We) and plastic components (Wp) since Wt = Wp+We.[28] The determination of the We/Wt ratio is straightforward from the load–unload curves, no need for any model application. The ratio cannot be affected by the shape of the stylus, the state of material (bulk or thin film), or the applied load, which are generally critical for the estimation of hardness and elastic modulus.[29] In the present, the average value of the We/Wt of the three coatings was obtained by calculating 15 curves. The result showed the We/Wt of the three coatings is 0.28, 0.43, 0.32, respectively. It illustrates that the coating B possesses a higher elasticity, which could be an advantage to improve the resistance against the deformation and the mechanical properties. **Figure 5** provided the morphology of the cross-section of the wear scar tested with the step profile The wear rate was calculated according to Equation (3):

$$k = \frac{S}{(L \times n)} \tag{3}$$

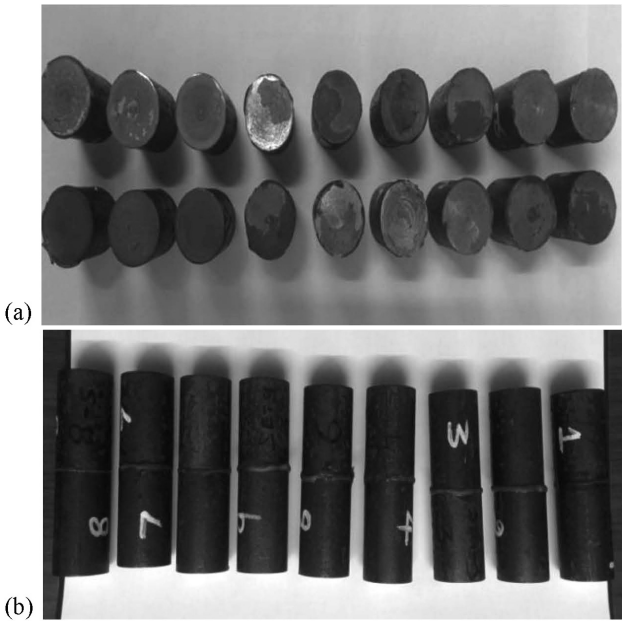

Figure 6: Coated specimens before and after adhesion strength

where S is that the area of the cross-section of the wear scar, L is that the load (N), n is the revolutions. The wear rate of the three coatings is shown in **Table 3**. The coating B has a higher wear resistance than the others, drawing this conclusion from its lower volume loss when tested. Coating B possesses the most effective wear resistance as a result of the dense structure, additional hard carbide, high fracture toughness, and sensible elasticity.

Those factors are all helpful to the coating resistance against a recurrent external force. The coating B was chosen to research the wear mechanism of the HVOF-sprayed 75Cr_3C_2-25NiCr coating seen in **Figure 7**. There is very little peeling, crack, and deformation on the worn surface. The scratches ensuing from the action of the abrasive particle and also the particle will be clearly recognized through an in-depth examination. For the Cr_3C_2-NiCr coating, an individual splat within the coating will be thought of as composites during which NiCr alloy could be a continuous matrix part with chromium carbides as the reinforcement hard phases. Because of the microhardness of metal carbides being abundant above that of NiCr matrix, the carbides are additional proof against cutting or gouging than matrix alloy phase. Consequently, the inorganic compound part with higher wear resistance would be removed at a lower rate, and also the carrying off of NiCr alloy binder also happens preferentially. Throughout the method of carrying, the high hardness of surface protuberance of the WC ball may insert into the as-tested coating surface, resulting in the removal of the metal binder-NiCr alloy and also the exposed Cr_3C_2 ceramic particles. Then, the exposed Cr_3C_2 particles suffered from shear removal as a result of the high-contact stress and cyclic stress, ensuing from the reciprocatory vibration and sliding wear method. As a result, the detached wear debris containing exhaust particles from the coatings and WC balls acted as abrasive particles, leading to severe, three-body abrasive wear at high temperature. The examination of the worn surface morphology recommended that the abrasive wear behavior of the HVOF sprayed Cr_3C_2-NiCr coating was dominated by the selective gouging or cutting of the NiCr binder matrix phase, followed by the removal of the carbide particles.

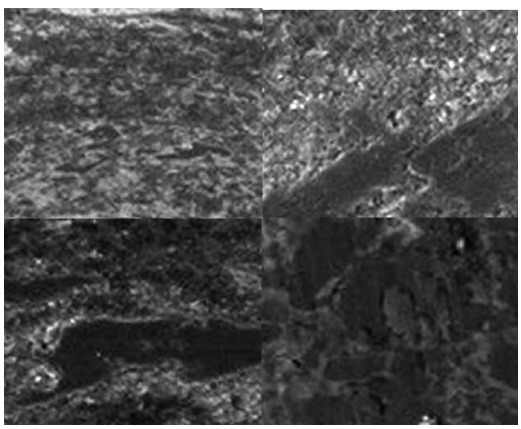

Figure 7: Micrographs of the worn surfaces of the coatings

4 CONCLUSIONS

HVOF-coated chromium-carbide-related coatings possessed a high microhardness, a low level of porosity, and a high level of adhesion strength. The powder feed had an evident effect on the coating substrate surface area and a mechanical property like the porosity, indention fracture toughness and microhardness. The coating sprayed at 35 g/min possessed a relatively lower porosity, a higher fracture toughness, and better elasticity. Thus, the HVOF-sprayed Cr_3C_2-NiCr coating using Hipojet 2700 system (Mec Jodhpur, India) had a suitable powder feed rate of 35 g/min. The wear test method showed that the HVOF sprayed 75Cr_3C_2-25NiCr carbide coatings possessed a good level of wear resistance at elevated temperature, which resulted from the steady friction coefficient and small crack and peeling and deformation on the coated worn surface area. The coating at the powder feed of 35 g/min had the best level of wear resistance due to the dense structure and sufficient fracture toughness.

5 REFERENCES

[1] M. Kaur, H. Singh, S. Prakash, High temperature corrosion studies of HVOF sprayed Cr3C2-NiCr coating on SAE-347H boiler steel, J. Therm Spray Technol., 18 (**2009**), 619–632, doi:10.1007/s11666-009-9371-9

[2] J. He, M. Ice, J. M. Schoenung, E. J. Lavernia, D. H. Shin, Thermal stability of nanostructured Cr3C2-NiCr coatings, J. Therm. Spray Technol., 10 (**2001**), 293–300, doi:10.1361/105996301770349385

[3] Z. Y. Hang, X. C. Lu, H. B. Luo, Tribological properties of rare earth oxide added Cr3C2-NiCr coatings, Appl. Surf. Sci., 253 (**2007**), 4377–4385, doi:10.1016/j.apsusc.2006.09.040

[4] C. J. Li, G. C. Ji, Y. Y. Wang, K. Sonoya, Dominant effect of carbide rebounding on the carbon loss during high velocity oxy-fuel spraying of Cr3C2 – NiCr, Thin Solid Films., 419 (**2002**), 137–143, doi:10.1016/S0040-6090(02)00708-3

[5] M. Magnani, P. H. Suegama, N. Espallargas, Influence of HVOF parameters on the corrosion and wear resistance of WC-Co coatings sprayed on AA7050 T7, Surf. Coat. Technol., 202 (**2008**), 4746–4757, doi:10.1016/j.surfcoat.2008.04.055

[6] G. Sun, Y. Zhang, C. Liu, K. Luo, X. Tao, P. Li, Microstructure and wear resistance enhancement of cast steel rolls by laser surface alloying NiCr–Cr3C2, Mater. Des., 31 (**2010**), 2737–2744, doi:10.1016/j.matdes.2010.01.021

[7] A. Milanti, H. Koivuluoto, P. Vuoristo, G. Bolelli, F. Bozza, L. Lusvarghi, Microstructural characteristics and tribological behavior of HVOF sprayed novel Fe based alloy coatings, Coatings., 4 (**2014**), 98–120, doi:10.3390/coatings4010098

[8] M. Manjunatha, R. S. Kulkarni, M. Krishna, Investigation of HVOF thermal sprayed Cr3C2 –NiCr cermet carbide coatings on erosive performance of AISI 316 molybdenum steel, Procedia Mater. Sci., 5 (**2014**), 622–629, doi:10.1016/j.mspro.2014.07.308

[9] S. Hong, Y. P. Wu, Q. Wang, G. B. Ying, Microstructure and cavitation silt erosion behavior of high velocity oxygen fuel HVOF sprayed Cr3C2 -NiCr coating, Surf. Coat. Technol., 225 (**2013**), 85–91, doi:10.1016/j.surfcoat.2013.03.020

[10] K. Murugan, A. Ragupathy, V. Balasubramanian, K. Sridhar, Optimizing HVOF spray process parameters to attain minimum porosity and maximum hardness in WC-10Co-4Cr coatings, Surf. Coat. Technol., 247 (**2014**), 90–102, doi:10.1016/j.surfcoat.2014.03.022

[11] Q. Wang, Z. H. Chen, L. X. Li, G. B. Yang, The parameters optimization and abrasion wear mechanism of liquid fuel HVOF sprayed bimodal WC-12Co coating, Surf. Coat. Technol., 206 (**2012**), 2233–2241, doi:10.1016/j.surfcoat.2011.09.071

[12] H. Fukumoto, The application of cermet coating on piston ring by HVOF, In Proceedings of the 14th International Thermal Spray Conference, Kobe, Japan, 22–26 May 1995.

[13] A. Mateen, G. C. Saha, T. I. Khan, F. A. Khalid, Tribological behaviour of HVOF sprayed near nanostructured and microstructured WC-17wt %Co coatings, Surf. Coat. Technol., 206 (**2011**), 1077–1084, doi:10.1016/j.surfcoat.2011.07.075

[14] C. W. Lee, J. H. Han, J. Yoon, M. C. Shin, S. I. Kwun, A study on powder mixing for high fracture toughness and wear resistance of WC-Co-Cr coatings sprayed by HVOF, Surf. Coat. Technol., 204 (**2010**), 2223–2229, doi:10.1016/j.surfcoat.2009.12.014

[15] G. C. Ji, C. J. Li, Y. Y. Wang, W. Y. Li, Microstructural characterization and abrasive wear performance of HVOF sprayed Cr3C2–NiCr coating, Surf. Coat. Technol., 200 (**2006**), 6749–6757, doi:10.1016/j.surfcoat.2005.10.005

[16] Y. F. Qiao, T. E. Fischer, D. Andrew, The effects of fuel chemistry and feedstock powder structure on the mechanical and tribological properties of HVOF thermal-sprayed WC–Co coatings with very fine structures, Surf. Coat. Technol., 172 (**2003**), 24–41, doi:10.1016/S0257-8972(03)00242-1

[17] ASTM C 633 Standard test method for adhesion or cohesion strength of thermal spray coatings, ASTM International, West Conshohocken, PA, USA, 1999.

[18] J. K. N. Murthy, K. S. Prasad, K. Gopinath, B. Venkataraman, Characterisation of HVOF sprayed Cr3C2-50 (Ni20Cr) coating and the influence of binder properties on solid particle erosion behavior, Surf. Coat. Technol. 204 (**2010**), 3975–3985, doi:10.1016/j.surfcoat.2010.04.069

[19] T. Sahraoui, N. E. Fenineche, Structure and wear behaviour of HVOF sprayed Cr3C2 -NiCr and WC–Co coatings, Materc. Des. 24 (**2003**), 309–313, doi:10.1016/S0261-3069(03)00059-1

[20] M. Mohanty, R. W. Smith, M. D. Bonte, J. P. Celis, E. Lugscheider, Sliding wear behaviour of thermally sprayed 75/25 Cr3C2-NiCr wear resistant coatings, Wear, 198 (**1996**), 261–266, doi:10.1016/0043-1648(96)06983-9

[21] P. Vuoristo, K. Niemi, A. Makela, T. Mantyla, Abrasion wear resistance of detonation gun sprayed carbide coatings, Proceedings of the 7th International Metallurgy and Materials Congress, Ankara, Turkey, 1993, 1295–1302

[22] M. Roy, A. Pauschitz, J. Bernardi, T. Koch, F. Franek, Microstructure and mechanical properties of HVOF sprayed nanocrystalline Cr3C2–25 (Ni20Cr) coating, Therm. Spray Technol., 15 (**2006**), 372–381, doi:10.1361/105996306X124374

[23] E. Celik, O. Culhaa, B. Uyulgan, N. F. Ak Azem, I. Ozdemir, A. Turk, Assessment of microstructural and mechanical properties of HVOF sprayed WC-based cermet coatings for a roller cylinder, Surf. Coat. Technol., 200 (**2006**), 4320–4328, doi:10.1016/j.surfcoat.2005.02.158

[24] J. Davenas, Modification of surfaces of polymers by ion bombardment for improvement of mechanical properties, Surf. Coat. Technol., 45 (**1991**), 229–235, doi:10.1016/0257-8972(91)90228-O

[25] L. Jacobs, M. M. Hyland, M. de Bonte, Comparative study of WC-cermet coatings sprayed via the HVOF and the HVAF process, Therm. Spray Technol., 7 (**1998**), 213–218, doi:10.1361/105996398770350954

[26] J. K. N. Murthy, B. Venkataraman, Abrasive wear behavior of WC–CoCr and Cr3C2–20(NiCr) deposited by HVOF and detonation spray processes, Surf. Coat. Technol., 200 (**2006**), 2642–2652, doi:10.1016/j.surfcoat.2004.10.136

[27] R. Bartali, V. Micheli, G. Gottardi, A. Vaccari, N. Laidani, Nano-indentation: Unload-to-load work ratio analysis in amorphous carbon films for mechanical properties, Surf. Coat. Technol., 204 (**2010**), 2073–2076, doi:10.1016/j.surfcoat.2009.11.002

[28] D. Beegan, S. Chowdhury, M. T. Laugier, Work of indentation methods for determining copper film hardness, Surf. Coat. Technol., 192 (**2005**), 57–63, doi:10.1016/j.surfcoat.2004.02.003

[29] N. Kiruchi, M. Kitagawa, A. Sato, E. Kusano, H. Nanto, A. Kinbara, Elastic and plastic energies in sputtered multilayered TiaTiN films estimated by nano indentation, Surf. Coat. Technol., 126 (**2000**), 131–135, doi:10.1016/S0257-8972(99)00670-2